IARJSET ISSN (O) 2393-8021, ISSN (P) 2394-1588

International Advanced Research Journal in Science, Engineering and Technology

Impact Factor 8.066 ⁘ Peer-reviewed & Refereed journal ⁘ Vol. 12, Issue 4, April 2025

DOI: 10.17148/IARJSET.2025.124116

Frequency Selective Surface Integrated GHz MIMO Antenna for Gain and Isolation Enhancement

Dr. Divya Gudapati[1], K. Sravanthi[2], K. Varshini[3], I. Jaswitha[4]

Assistant Professor, Department of Electronics and Communication Engineering, Bapatla Women's Engineering College, Bapatla, A.P, INDIA- 522101[1]

U. G Student, Department of Electronics and Communication Engineering, Bapatla Women's Engineering College, Bapatla, A.P, INDIA-522101[2,3,4]

Abstract: This work presents an innovative approach to enhancing GHz-range MIMO antenna systems through the implementation of an advanced Frequency Selective Surface (FSS) framework. Leveraging modern computational methodologies and the principles of metamaterials, the design targets substantial improvements in both gain and isolation performance metrics. The antenna prototype is realized on a silicon dioxide substrate, measuring 70 × 76 mm^2 with a thickness of 1.52 mm. Central to the design is a novel FSS unit cell architecture, inspired by metamaterial behaviour, which enables precise frequency filtration and refined electromagnetic wave manipulation. To elevate the antenna's overall efficiency, a dual-layer FSS strategy is adopted. One FSS layer is placed at the rear of the antenna to reflect reverse-propagating waves, thereby amplifying directional gain. A second FSS layer is strategically embedded between the MIMO elements, effectively mitigating mutual coupling and enhancing radiation quality. Simulation data confirms the efficacy of this configuration, showcasing an increase in antenna gain from 7.6 dBi to 10.6 dBi and an isolation performance exceeding 85 dB. These improvements underscore the potential of the proposed structure as a forward-looking solution for next-generation wireless systems that operate in the high-frequency GHz domain.

Keywords: Frequency Selective Surface (FSS), Gain Enhancement, Isolation Improvement, FSS reflector.

I. INTRODUCTION

Frequency Selective Surfaces (FSS) represent a foundational concept in electromagnetic (EM) engineering, comprising two-dimensional periodic structures made up of metallic patches or apertures printed on a dielectric substrate [1]. These structures exhibit selective transmission and reflection properties at specific resonant frequencies. When an incident plane wave aligns with the resonance of the FSS elements, it is either reflected or transmitted fully or partially depending on the configuration of the array [2]. This frequency-dependent response allows FSS to function as spatial filters, enabling or blocking electromagnetic waves at designated frequencies in free space. Typically classified as meta surfaces, FSS structures exhibit predominantly electric responses, as electrical polarization is often sufficient to achieve desired filtering characteristics. Constructed using thin, planar metallic patterns in periodic arrangements, these elements are designed such that their physical thickness is negligible relative to the wavelength but remains significantly larger than the metal's skin depth [3].

This facilitates the modelling of FSS as a thin layer of ideal, conductive resonators. Complementary FSS designs [4] based on apertures rather than patches are subject to design constraints, particularly when the cavity size approaches that of the unit cell, as in wire-mesh topologies. Common designs utilize square or hexagonal wire meshes [5], referred to as capacitive grids. These resonant structures give rise to side lobes in both transmitted and reflected fields, a hallmark feature of conventional FSS. However, meta surfaces featuring unit cells and resonant elements that are subwavelength in scale can effectively suppress grating lobes, which is particularly advantageous at terahertz frequencies. For this reason, FSS operating in the terahertz domain are often synonymous with meta surfaces.

In parallel, the evolution of wireless communication has been significantly driven by Multiple-Input Multiple-Output (MIMO) technology [6], which employs multiple antennas at both the transmitting and receiving ends. MIMO systems enhance communication reliability and throughput by exploiting multipath propagation through spatial multiplexing. This approach addresses growing demands for higher data rates, lower latency, expanded channel capacity, and improved spectral efficiency, all in accordance with Shannon's capacity limits [7].

IARJSET ISSN (O) 2393-8021, ISSN (P) 2394-1588

International Advanced Research Journal in Science, Engineering and Technology

Impact Factor 8.066 ⧖ Peer-reviewed & Refereed journal ⧖ Vol. 12, Issue 4, April 2025

DOI: 10.17148/IARJSET.2025.124116

MIMO has become integral to a broad spectrum of wireless technologies, including 3G, 4G, LTE, Wi-Fi, WLAN, WiMAX, and plays a pivotal role in the development of 5G and beyond. Operating across multiple frequency bands, MIMO provides strong signal integrity, high isolation, and substantial data throughput capabilities essential for the transmission of high-bandwidth content like HD video and real-time streaming. The underlying principle involves transmitting and receiving data streams over different paths using multiple antenna elements, with each pair characterized by a channel coefficient representing the propagation environment.

In contemporary wireless systems, antennas are fundamental to ensuring effective communication. Two critical metrics gain and isolation largely determine antenna performance. Gain enhancement focuses on increasing the antenna's ability to direct RF energy in preferred directions, which is vital for long-distance links and beamforming technologies. This is often achieved using methods like parasitic elements, electromagnetic bandgap (EBG) structures, and metamaterials [8]. On the other hand, isolation enhancement is crucial in multi-antenna arrangements to mitigate mutual coupling [9], which can degrade system performance by increasing interference, reducing radiation efficiency, and distorting beam patterns. Common techniques for improving isolation include decoupling networks, neutralization lines, and defected ground structures (DGS), which suppress unwanted coupling between closely spaced antenna elements [10].

Together, these technologies FSS, MIMO, and advanced antenna design techniques pave the way for high-performance, next-generation wireless communication systems capable of meeting the growing demands of data-driven applications.

II. DESIGNING APPROACH OF FSS BASED HIGH-GAIN & HIGH ISOLATION ANTENNA

This section delves into the structural configuration of both the antenna and the Frequency Selective Surface (FSS), outlining the underlying operational mechanisms. It also provides a concise analysis of the individual performance characteristics of the antenna and the FSS. The evaluation of these characteristics is carried out using CST (Computer Simulation Technology), a widely recognized electromagnetic simulation tool.

EVOLUTION STAGES OF ANTENNA

The monopole patch element is positioned a top a Silicon Dioxide substrate, characterized by a relative permittivity (ϵ_r) of 3.9 and a loss tangent of 0.001. Given the total antenna structure size of $40 \times 20 \times 1.52$ mm³, which indicates a compact microstrip design, a unique approach would be to maximize performance within this strict volume using space-efficient innovations. The layout features a combination of precision-engineered slots and stubs, strategically introduced to optimize the antenna's performance across its operating band. A complete ground plane is located on the reverse side of the substrate, fabricated from gold with a thickness of 0.036 mm, contributing to enhanced signal stability and improved electromagnetic behaviour.

The optimized antenna geometry is the result of iterative design refinements, carefully tailored to achieve the targeted performance metrics.

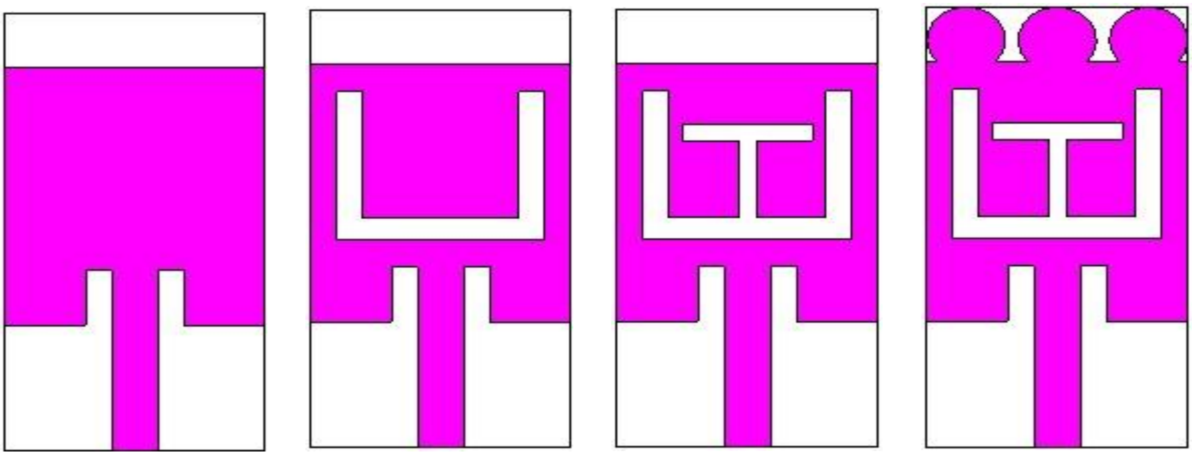

(a) Stage 1 **(b) Stage 2** **(c) Stage 3** **(d) Prop Ant**

Fig 1. Evolution of the Proposed Antenna

Design Stage 1: Initial Development of the Rectangular Patch Antenna

DOI: 10.17148/IARJSET.2025.124116

The design process begins with the formulation of a basic rectangular patch antenna, serving as the foundational structure for the overall configuration. The patch dimensions, length and width are derived using standard design equations as outlined in [11].

$$\text{Width of the patch, } W = \frac{c}{2fo\sqrt{\text{€}r+1/2}} \quad \ldots\ldots\ldots\ldots\ldots (1)$$

Effective dielectric constant,

$$\text{€eff} = \frac{\text{€}r+1}{2} + \frac{\text{€}r-1}{2}\left[1 + 12\frac{h}{w}\right]^{-\frac{1}{2}} \quad \ldots\ldots\ldots\ldots.. (2)$$

$$\text{Effective Length, } Leff = \frac{c}{2fo\sqrt{\text{€}eff}} \quad \ldots\ldots\ldots\ldots. (3)$$

$$\text{Extent in Length, } \Delta L = 0.412h + \frac{(\text{€}eff+0.3)(\frac{W}{h}+0.264)}{(\text{€}eff-0.258)(\frac{W}{h}+0.8)} \quad \ldots\ldots\ldots\ldots\ldots (4)$$

This initial configuration is tuned to resonate at approximately 5.9 GHz, as illustrated in Fig. 2, establishing the baseline performance for subsequent design enhancements.

Design Stage 2: Etching of the U-Shaped Slot

In this stage of the design process, a U-shaped slot is etched into the patch, as depicted in Fig. 1(b). This U-shaped slot is an innovative modification that enhances the antenna's performance by refining its resonance characteristics, all while maintaining a compact size. The addition of this slot enables resonance at 4.7 GHz, as depicts in Fig. 2, contributing to the antenna's improved operational bandwidth.

Design Stage 3: Etching of the T-Shaped Slot

In this phase of the design, a T-shaped slot is etched into the antenna, as shown in Fig. 1(c). The T-shaped configuration is a vital design enhancement that significantly improves the antenna’s performance and functionality. This modification introduces resonances at 4.14 GHz and 9.7 GHz, achieving return losses of -24 dB and -12 dB, respectively, thereby enhancing the antenna’s overall efficiency and frequency response.

Design Stage 4: Incorporation of Circular Parasitic Stubs

Introducing circular parasitic stubs in the final stage of a rectangular microstrip patch antenna design is a known technique to enhance bandwidth, improve impedance matching, or modify the radiation pattern. This addition significantly alters the antenna's resonance behaviour, enabling it to resonate at two distinct frequencies: 5.5 GHz and 9 GHz. The modified design achieves return losses of -36 dB and -14 dB at these frequencies, respectively, marking a notable improvement in performance and signal efficiency.

The structure of the recommended antenna is given in Fig. 2 and the dimensions are listed.

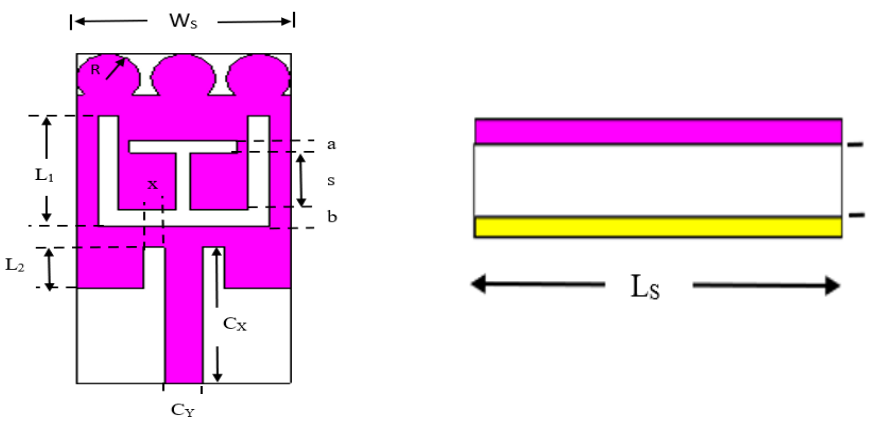

(a) Top View (b) Front View

DOI: 10.17148/IARJSET.2025.124116

Fig 2. The proposed antenna configuration is illustrated with both top and side views, highlighting key structural parameters (all dimensions in mm): L_S = 40, W_S = 20, a = 1.50, b = 2.8, S = 7, L_1 = 13.50, L_2 = 5, x = 2, R = 3, C_X = 16.50, C_Y = 3.60, and substrate thickness T = 1.52 mm.

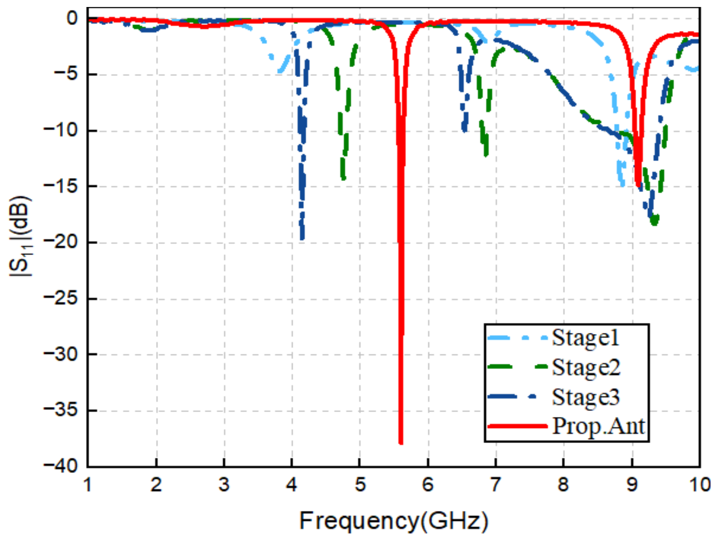

Fig 3. Return Loss versus Frequency Plot

Fig 3. presents the return loss profile of the antenna, highlighting its efficiency in minimizing signal reflections and ensuring optimal impedance alignment over the designated frequency spectrum.

2.2. Optimized FSS-1 Architecture for Forward Gain Enhancement:

The proposed Frequency Selective Surface (FSS-1) features an innovative unit cell design characterized by a 20 × 20 mm^2 footprint and fabricated on a 1.52 mm thick FR-4 substrate with lossy dielectric properties. The full FSS surface is realized by assembling a 4 × 4 matrix of these unit cells, resulting in a composite structure measuring 120 × 120 mm^2. Each unit cell consists of a main square patch, precisely etched with four internal square slots that impart the surface with superior frequency filtering capabilities. This configuration enables the FSS to exert precise control over incident electromagnetic waves, particularly by reflecting backward radiation away from the antenna, thereby increasing the effective gain in the desired direction. The functional behaviour of the FSS, including its selective transmission and reflection properties across the GHz spectrum, aligns with established electromagnetic principles discussed in [12]. The compact and efficient design of FSS-1 shown in Fig 4, makes it a valuable component for modern antenna systems requiring enhanced directional performance without increasing overall dimensions.

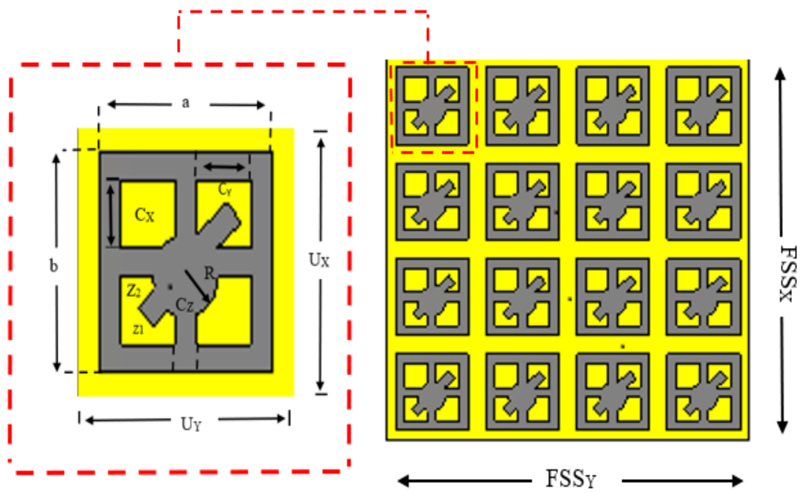

Fig 4. Geometrical configuration of proposed FSS-1. FSS_X = 60, FSS_Y = 60, U_X = 20, U_Y = 20, a=16, b=16, C_X=12, C_Y=12, C_2=2, Z_1=2, Z_2=2 (unit in mm).

IARJSET ISSN (O) 2393-8021, ISSN (P) 2394-1588

International Advanced Research Journal in Science, Engineering and Technology

Impact Factor 8.066 ⪴ Peer-reviewed & Refereed journal ⪴ Vol. 12, Issue 4, April 2025

DOI: 10.17148/IARJSET.2025.124116

2.3. Integration of FSS with Antenna for Gain Enhancement

This section highlights the operational concept behind integrating a Frequency Selective Surface (FSS) with the antenna to achieve notable performance gains. The proposed FSS structure is strategically placed beneath the antenna element is given in Fig. 5, separated by an optimized vertical spacing of 12 mm (denoted as *s*) to ensure effective electromagnetic interaction. This configuration is designed to exploit the reflective properties of the FSS, which helps redirect the backward propagating waves toward the main lobe, thereby strengthening the antenna's forward radiation and improving overall gain. The spatial placement of the FSS plays a critical role in phase alignment and constructive interference, making it a key factor in the observed performance improvements. This technique provides a passive, low-profile, and efficient method to boost antenna characteristics without introducing complex circuitry or active components.

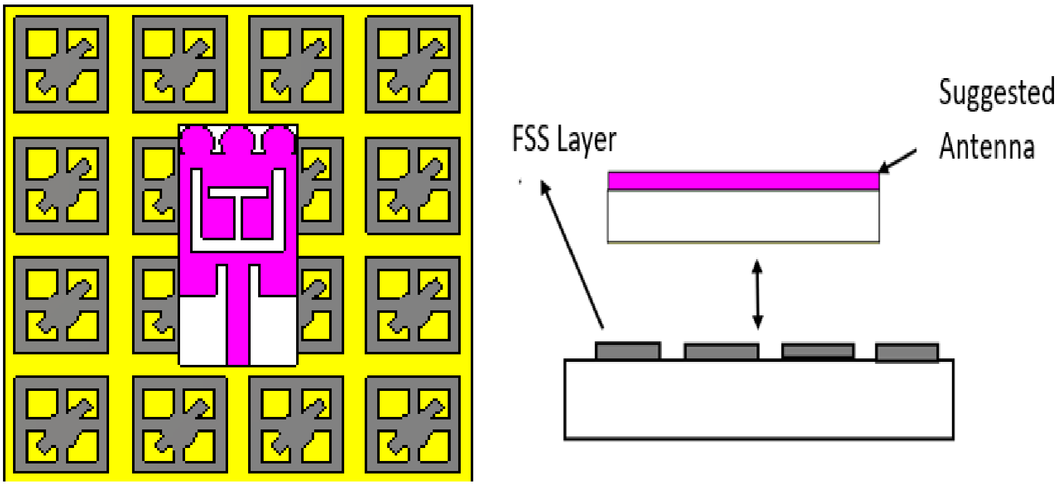

Fig 5. FSS -1 with Single Antenna

2.4. Design of FSS-2 Design for Isolation Enhancement:

The Frequency Selective Surface (FSS-2) unit cell is structured within a square footprint of 24 × 24 mm^2 and is fabricated on a lossy FR-4 substrate with a dielectric thickness of 1.52 mm. To construct the complete surface, a 4×4 array of these unit cells is arranged, resulting in an overall dimension of 48 × 48 mm^2 for the FSS-2 layer, depicted in Fig 6.

Each unit cell features a primary square patch, centrally positioned, from which five smaller square sections are strategically etched. Four of these are symmetrically removed from each corner of the main patch, while the fifth square is etched precisely at the centre. This etching pattern is tailored to modulate electromagnetic response characteristics, enabling the desired frequency-selective behaviour. The S-parameter results, which reflect the transmission and reflection performance, further validate the electromagnetic functionality of this multi-layered FSS design.

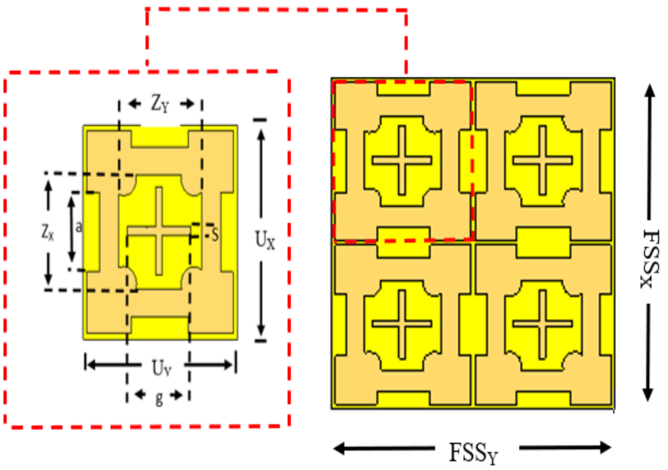

Fig 6. Geometrical configuration of proposed FSS-2. FSS_X = 48, FSS_Y = 48, U_X = 24, U_Y = 24, Z_X=23, Z_Y=23, a=9, b=1.9, g=5, S=1 (unit in mm).

DOI: 10.17148/IARJSET.2025.124116

III. DESIGNING APPROACH OF MIMO ANTENNA

The design of the proposed 2 × 2MIMO antenna system featuring slotted patch elements are depicted in Fig 7. This antenna configuration marks a progressive advancement over conventional rectangular patch designs, incorporating strategic slotting to enhance performance characteristics such as bandwidth and isolation. The dimensional parameters of the MIMO structure are directly derived from the optimization of its single-element counterpart, ensuring consistency in resonant behaviour. The complete MIMO antenna exhibits compact dimensions of 70 × 76 × 1.52 mm^3, making it notably smaller than many conventional MIMO antennas, while still delivering robust functionality suited for modern wireless applications.

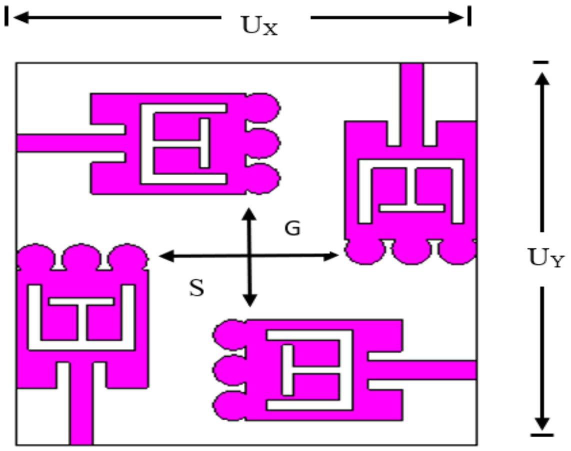

Fig 7. Schematic view of the proposed MIMO antenna.
Dimensions: $U_X = 70$, $U_Y = 76$, S = 18.50, G = 16 (unit in mm).
The return loss plot of the proposed MIMO antenna is shown in Fig 8.

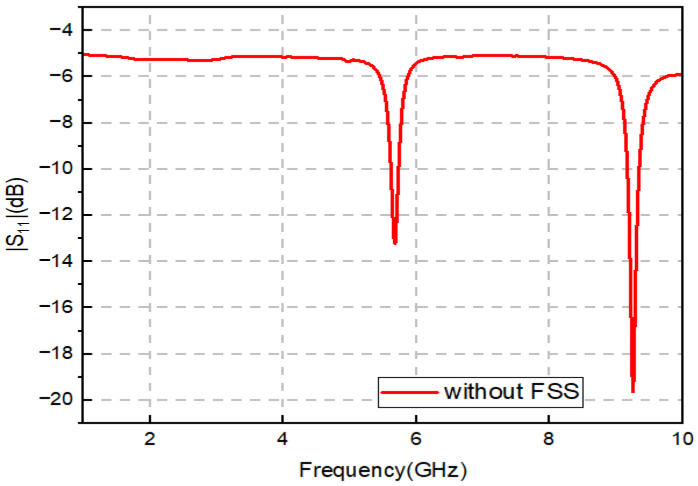

Fig 8. Return Loss Plot of the 2 × 2 proposed MIMO antenna

The antenna, when combined with the Frequency Selective Surface (FSS), exhibits strong simulated performance across its designated frequency range. The reflection coefficient (S11) consistently remains below –10 dB, reflecting efficient impedance matching and reduced signal reflection.

Integration of Single Side FSS-2 Layer

The single side FSS-2 layer is designed for the isolation enhancement shown in Fig. 9(a). FSS 2 layer is etched on side of the wall placed between the adjacent elements of the MIMO configuration. With single side FSS-2 layer the impedance matching is not attained shown in Fig. 9(b). This can be compensated with etching FSS-2 layer on other side of the wall, thereby originating double sided FSS.

IARJSET ISSN (O) 2393-8021, ISSN (P) 2394-1588

International Advanced Research Journal in Science, Engineering and Technology

Impact Factor 8.066 ⁜ Peer-reviewed & Refereed journal ⁜ Vol. 12, Issue 4, April 2025

DOI: 10.17148/IARJSET.2025.124116

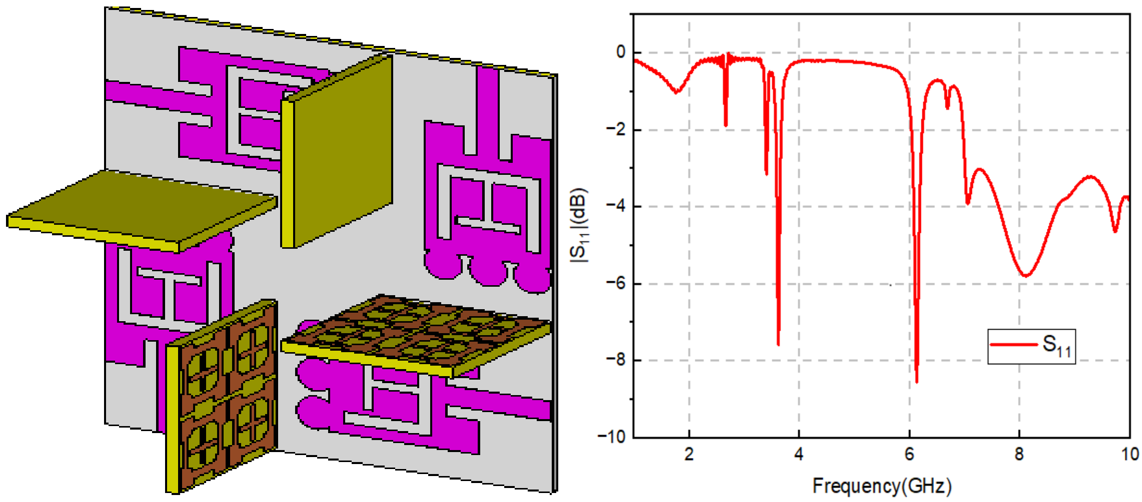

(a) Single Sided FSS layer 2 (b) Return Loss Plot

Fig 9. MIMO Antenna Configuration with Single Sided FSS – 2

Double Side FSS-2 layer

The double side FSS-2 layer is designed for the isolation enhancement shown in Fig. 10(a). The FSS-2 layer is etched on both sides of the wall and is strategically positioned between the MIMO antenna elements to effectively reduce mutual coupling, thereby enhancing isolation and overall system performance. This placement acts as an electromagnetic barrier. The double side FSS-2 layer is constructed is designed for the isolation improvement for overall antenna. For the isolation improvement four double side FSS-2 layers are constructed between the MIMO antenna. The return loss plot for double sided FSS 2 layer is depicted in Fig 10(b).

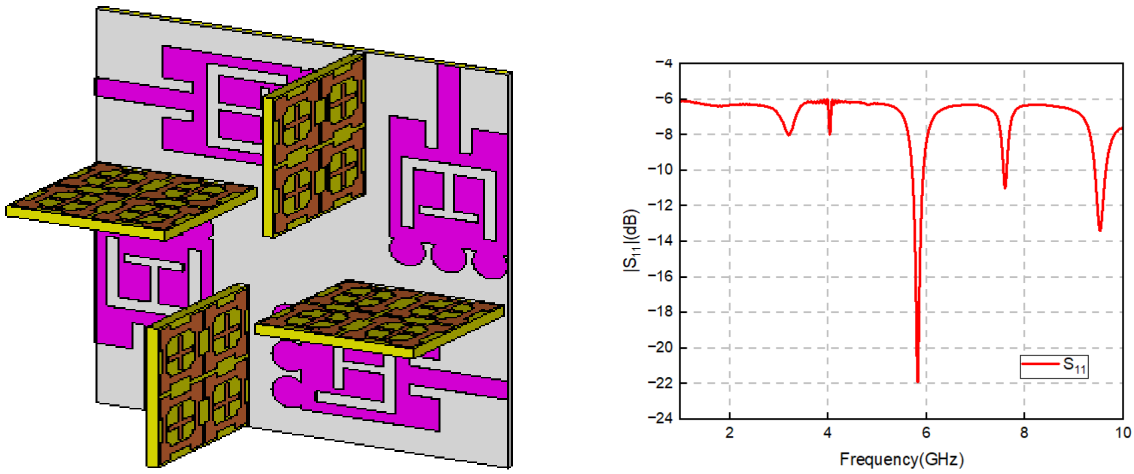

(a) Double Sided FSS 2 Layer (b) Return Loss Plot

Fig 10. MIMO Antenna Configuration with Double Sided FSS – 2

The obtained resonant frequencies for the above proposed MIMO antenna along with double sided FSS-2 layer are resonates at 5.9, 7.7, 9.6 GHz.

Proposed MIMO Antenna With FSS-1 & FSS-2

The proposed 2 × 2 MIMO Antenna with FSS-1 & FSS-2 layers are designed for the gain and Isolation enhancement shown in Fig 11. The corresponding return loss plot is shown in Fig 12.

IARJSET ISSN (O) 2393-8021, ISSN (P) 2394-1588

International Advanced Research Journal in Science, Engineering and Technology

Impact Factor 8.066 ⁜ Peer-reviewed & Refereed journal ⁜ Vol. 12, Issue 4, April 2025

DOI: 10.17148/IARJSET.2025.124116

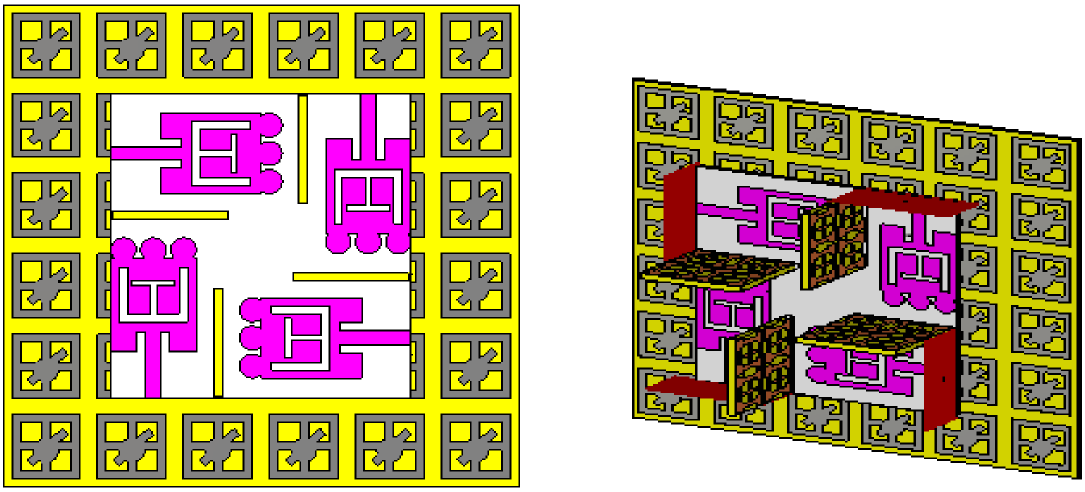

(a) Top View (b) Isometric View

Fig 11. Proposed MIMO Antenna with FSS 1 & FSS 2 Layers

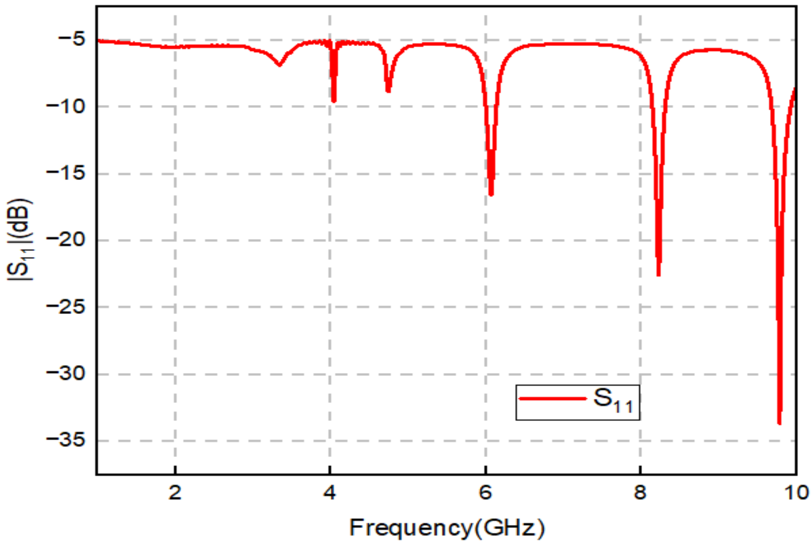

Fig 12. Return Loss Plot of the proposed MIMO antenna with FSS-1 & FSS-2

IV. RESULT

Fig 13. The Gain versus Frequency Plot indicates that the proposed antenna has the four stags, the related results are show in Fig 13. The stage 1 resonant at 8.8 GHz, corresponding gain is 4.1 dBi. Adding a U shape slot resonant at 4.7 GHz, gain of the antenna is 4.2 dBi. Moving to a T shape slot antenna resonant at 4.14 GHz, gain is 3.3 dBi. To overcome this type of issue to go for the stage 4 (Prop. Ant) antenna resonant at 5.7 GHz, achieve gain at 6.2 dBi.

DOI: 10.17148/IARJSET.2025.124116

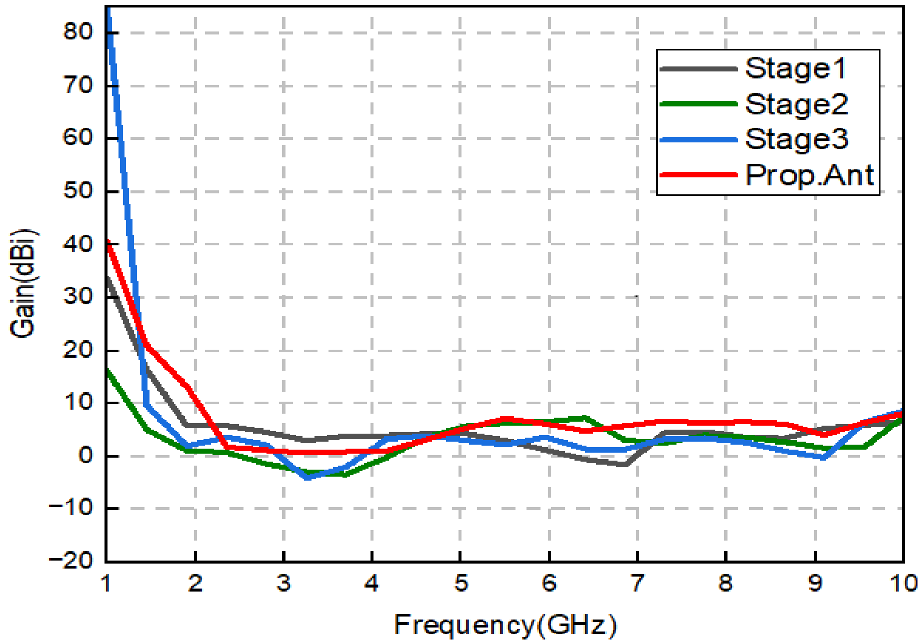

Fig 13. Gain versus Frequency Plot of Evolution Stages of Antenna

The return loss plot of the without & with Ant is depicted in Fig 14. The antenna, in its unaltered configuration, demonstrates resonance at 1.65 GHz, indicating effective energy radiation at this frequency. This setup achieves a measurable gain, expressed in dBi, reflecting its directional performance and efficiency within the resonant band. The with antenna has achieve the double band at 9.3 & 5.8 GHz, corresponding gains are 6.22 & 7.99 dBi.

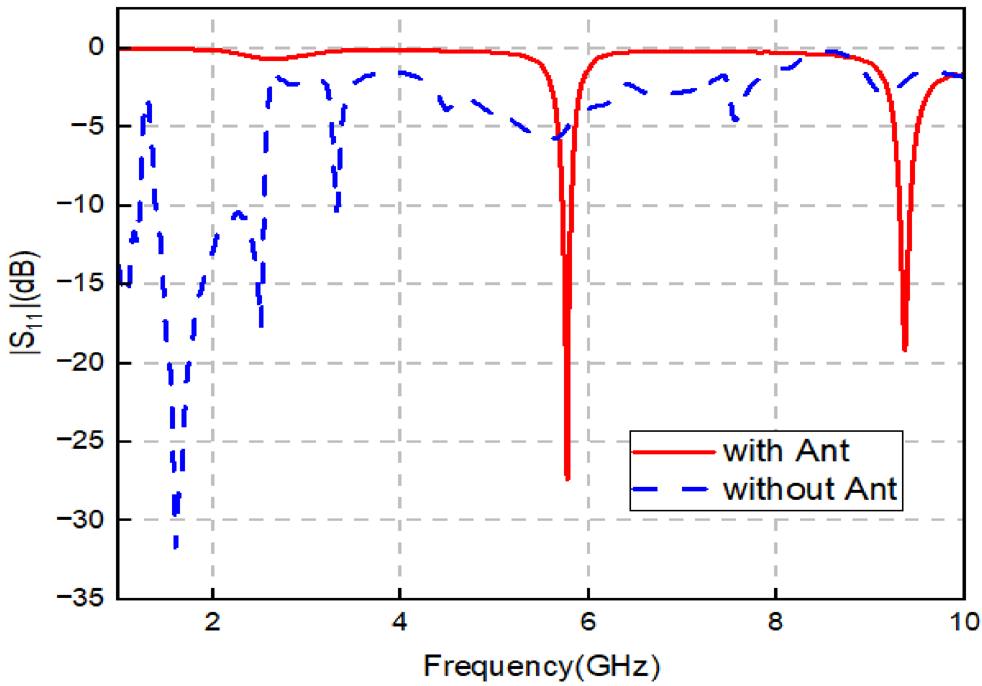

Fig 14. Return Loss versus Frequency Plot of without & with Ant

The isolations of the proposed MIMO antenna are S_{21}=59, S_{31}=65, S_{41}=62, S_{23}=71, S_{24}=78, S_{34}=64 as Shows in the below Fig 15.

IARJSET
ISSN (O) 2393-8021, ISSN (P) 2394-1588
International Advanced Research Journal in Science, Engineering and Technology
Impact Factor 8.066 ⁎ Peer-reviewed & Refereed journal ⁎ Vol. 12, Issue 4, April 2025
DOI: 10.17148/IARJSET.2025.124116

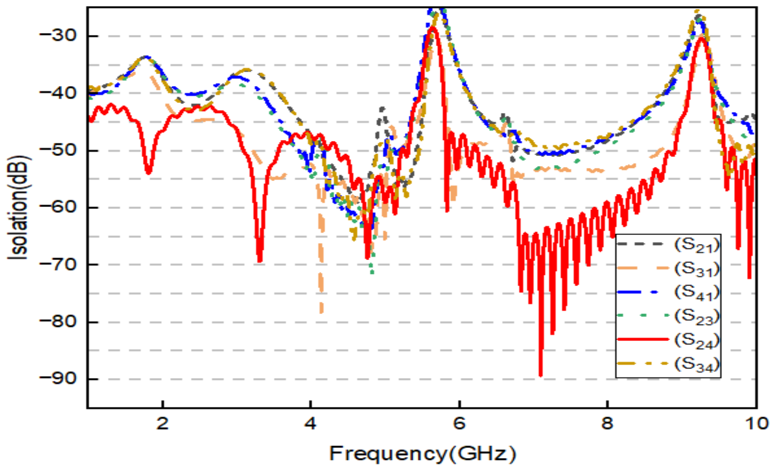

Fig 15. Isolations of the proposed MIMO antenna

The below Fig 16 shows the double side FSS-2 is resonant frequency at 5.8 GHz, the corresponding isolations are shown in above Fig(c), S_{21}=75, S_{31}=76, S_{41}=66, S_{23}=58, S_{24}=73, S_{34}=79.

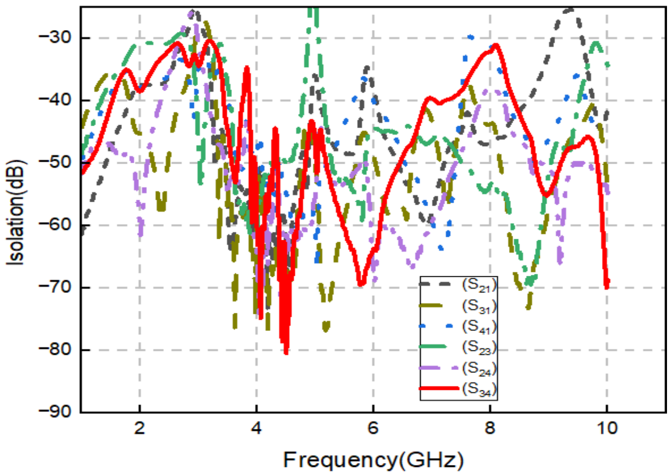

Fig 16. Depicts the isolations of the double Side FSS-2 layer

The below Fig 17. shows the measured isolation values are S21 = 66 dB, S31 = 85 dB, S41 = 61 dB, S23 = 63 dB, S24 = 74 dB, and S34 = 69 dB.

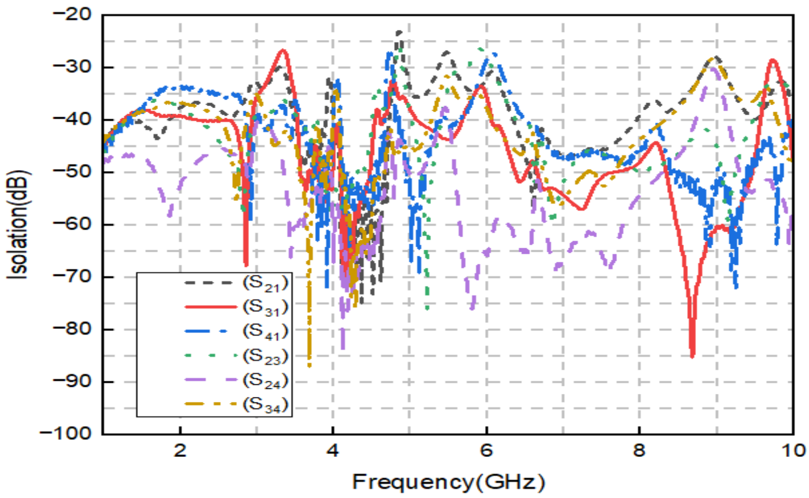

Fig 17. Isolations of the Proposed MIMO Antenna With FSS-1 & FSS-2

IARJSET ISSN (O) 2393-8021, ISSN (P) 2394-1588

International Advanced Research Journal in Science, Engineering and Technology

Impact Factor 8.066 ⋇ Peer-reviewed & Refereed journal ⋇ Vol. 12, Issue 4, April 2025

DOI: 10.17148/IARJSET.2025.124116

The E & H fields of the Proposed MIMO Antenna With FSS-1 & FSS-2 is shown in Fig 18.

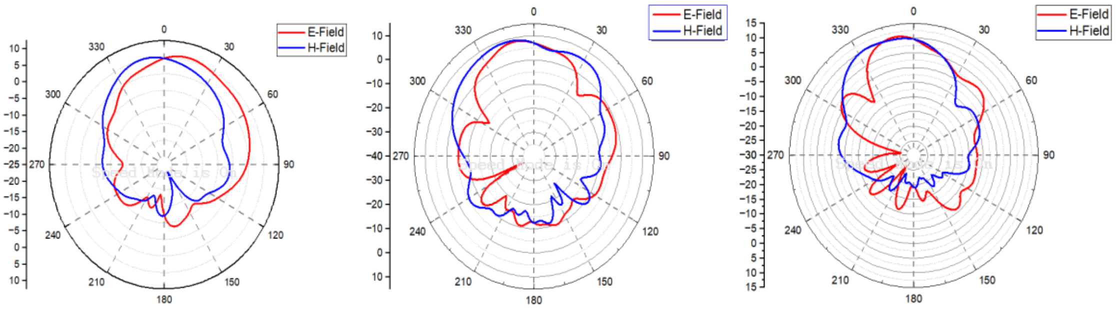

(a) (b) (c)

Fig 18. Radiation pattern of proposed antenna with FSS at (a) 6.06 GHz (b) 8.22 GHz.(c) 9.78 GHz

V. CONCLUSION

The designed rectangular patch antenna with a center slot provides a gain of 6.2 dBi, showing improved performance due to better current flow and radiation. Integrating an FSS-1 layer increases the gain to 8.0 dBi. Moving to a four-element setup without any FSS layer, the gain rises to 9.14 dBi, and the isolation is 59.20 dB, showing better performance. A 2 × 2 MIMO antenna with a double-sided FSS-2 layer provides high isolation 79 dB. The proposed MIMO antenna by integrating FSS-1 & FSS-2 layers results in high gain of 10.6 dBi and the best isolation at 85.2 dB.

REFERENCES

[1]. B. A. Munk, *Frequency Selective Surfaces: Theory and Design*. New York, NY, USA: Wiley-Interscience, 2000.
[2]. T. K. Wu, *Frequency Selective Surface and Grid Array*. New York, NY, USA: Wiley-Interscience, 1995.
[3]. B. A. Munk, *Frequency Selective Surfaces: Theory and Design*. New York, NY, USA: Wiley-Interscience,2000.
[4]. T. K. Wu, *Frequency Selective Surface and Grid Array*. New York, NY, USA: Wiley-Interscience, 1995.
[5]. C. L. Holloway, E. F. Kuester, J. A. Gordon, J. O'Hara, J. Booth, and D. R. Smith, "An overview of the theory and applications of metasurfaces: The two-dimensional equivalents of metamaterials," *IEEE Antennas and Propagation Magazine*, vol. 54, no. 2, pp. 10–35, Apr. 2012.
[6]. C. L. Holloway, E. F. Kuester, J. A. Gordon, J. O'Hara, J. Booth, and D. R. Smith, "An overview of the theory and applications of metasurfaces: The two-dimensional equivalents of metamaterials," *IEEE Antennas and Propagation Magazine*, vol. 54, no. 2, pp. 10–35, 2012.
[7]. A. A. Kishk, "High-Gain Antennas for Wireless Communications," *IEEE Antennas and Propagation Magazine*, vol. 52, no. 5, pp. 106–115, 2010.
[8]. C. E. Shannon, "A mathematical theory of communication," *Bell System Technical Journal*, vol. 27, no. 3, pp. 379–423, Jul. 1948.
[9]. E. G. Larsson, O. Edfors, F. Tufvesson, and T. L. Marzetta, "Massive MIMO for next generation wireless systems," *IEEE Communications Magazine*, vol. 52, no. 2, pp. 186–195, Feb. 2014.
[10]. M. M. Shalaby, M. A. Z. Al-Saleh, and K. F. Lee, "Metamaterials and their applications in antenna design," *Progress In Electromagnetics Research*, vol. 115, pp. 233-267, 2011.
[11]. Khalid H, Awan WA, Hussain M, Fatima A, Ali M, Hussain N, et al. Design of an Integrated Sub-6 GHz and mm Wave MIMO Antenna for 5G Handheld Devices. Appl. Sci. 2021; 11:8331.
[12]. K. A. Zaki, M. I. K. Eltawil, and M. A. Al-Nuaimi, "Isolation enhancement techniques for multi-antenna systems: A survey," *IEEE Access*, vol. 8, pp. 35447–35463, 2020.
[13]. H. S. S. S. Geyer, M. S. R. L. M. R. De Lima, and M. G. de Almeida, "Design of a compact broadband antenna with a complete ground plane for wireless communication systems," *IEEE Transactions on Antennas and Propagation*, vol. 60, no. 9, pp. 4416–4423, Sept. 2012.
[14]. B. A. Munk, *Frequency Selective Surfaces: Theory and Design*. New York, NY, USA: Wiley-Interscience, 2000.